Journal of Sol-Gel Science and Technology (2022) 104:580–587
https://doi.org/10.1007/s10971-022-05766-4

INVITED PAPER: NANO-STRUCTURED MATERIALS (PARTICLES, FIBERS, COLLOIDS, COMPOSITES, ETC.)

Colloidal dispersion of chiral layered hydroxide salt (LHS) nanocrystals exhibiting chiroptical response

Yasuaki Tokudome[1] · **Akihiro Koyama**[1] · **Hidenobu Murata**[1] · **Kenji Okada**[1] · **Atsushi Nakahira**[1] · **Shigenori Nishimura**[2] · **Masahide Takahashi**[1]

Received: 1 February 2022 / Accepted: 2 March 2022 / Published online: 4 April 2022

Abstract

Chiral inorganic materials have attracted increasing attention in the fields such as catalysis, electronics, photonics, and sensing. A new class of functional materials with chirality is extensively explored. Herein, we demonstrate the synthesis of nanometric nickel layered hydroxide salt (Ni-LHS) modified with chiral amino acids, (D- or L-) phenylalanine (PHE). An alkalization reaction in a starting mixture of nickel-phenylalanine aqua complexes was induced by using propylene oxide, leading to intercalate and adsorb phenylalanine on the surface and into the interlayers of Ni-LHS in an in-situ manner. The chiral molecules also act as surface modifier to inhibit the extensive crystal growth and aggregation, to form Ni-LHS with a diameter of 2–3 nm in a state of stablly-suspended in a solvent. It was also found that Ni-LHS exhibit induced circular dichroism (ICD) in the spectral range of *d-d* transitions of Ni(II) metal centres. The layered nanomaterials with chiroptical response demonstrated here is a promising option as an advanced adsorbent for detection of molecules.

Graphical abstract

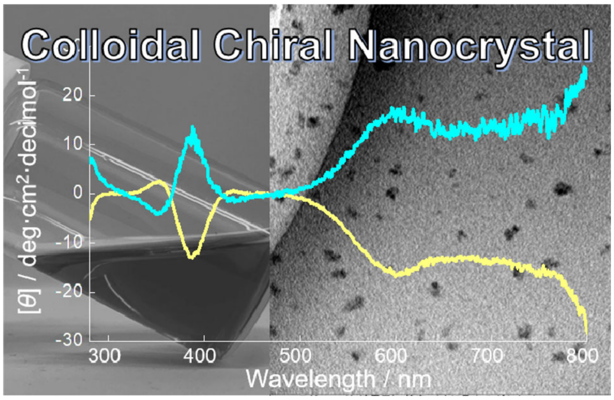

Keywords Layered hydroxide salts · Epoxide-mediated alkalinization · Sol · Colloid · Circular dichroism · Chirality

---

Supplementary information The online version contains supplementary material available at https://doi.org/10.1007/s10971-022-05766-4.

✉ Yasuaki Tokudome
tokudome@mtr.osakafu-u.ac.jp

[1] Department of Materials Science, Osaka Prefecture University 1-1, Gakuencho, Naka-ku, Sakai, Osaka 599-8531, Japan

[2] Department of Applied Life Sciences, Graduate School of Life and Environmental Sciences, Osaka Prefecture University, 1-1 Gakuencho, Naka-ku, Sakai, Osaka 599-8531, Japan

Highlights

- Synthesis of nanometric nickel layered hydroxide salt accommodating chiral amino acids is achieved.
- Epoxide-mediated alkalization reaction is adopted for the synthesis of the stable sol of the nano hydroxide.
- The material is found to exhibit induced circular dichroism (ICD) in visible light range.

1 Introduction

Chirality is a geometric feature of a structure which cannot be superimposed on its mirror image. Chiral recognition typically occurring in nature and living systems is crucial on fundamental and application aspects in the cutting-edge fields of biology, separation [1, 2], and asymmetric catalysis [3]. Chirality on a solid surface is especially attracting because a surface to be adsorbed by chiral molecules potentially show chiralities at molecular and organization (macro) levels [4]. For examples in heterogeneous catalysis, transition metal centres complexed with chiral ligands are immobilized on solid surfaces, such as mesoporous silica [5–7], smectites [8], Zr-bases salt [9], and CNT [10].

Interestingly, a solid surface for the immobilization of chiral molecules can, in some cases, work as more than support materials and enhance properties, when electronic and/or magnetic interactions between the surface and chiral molecules are properly designed. Circular dichroism (CD) from quantum dots (QDs) is a kind of the enhanced chiral response [11]. CdS, CdSe, and HgS QDs prepared in the presence of chiral surfactant molecules are reported to exhibit CD signals related to a modulated excitonic band structure [12–14]. In addition, semiconductors with crystallographic and morphological chiralities showing much stronger chiroptical effects have been demonstrated in these systems [15]. The chiromorphological features are also demonstrated in metal nanoparticles, including Te, Se, Ag, and Au [16], where CD is further enhanced by being coupled with plasmon-enhanced absorption [17, 18].

One of the promising applications taking advantage of these chiroptical responses is sensing/detection of molecules [19, 20]. Circular dichroism (CD) by introducing a strong specific physical interaction with analytes has been widely used to study biopolymers such as proteins, nucleic acids, and polysaccharides [21, 22]. The development of inorganic chiral nanomaterials with a capability of loading analytes at a high concentration is of high priority to this end. On the other hand, nanomaterials exhibiting chiroptical response are still limited in several metals and metal sulfides, where only the surface of crystals adsorb analytes to be detected. It is required to explore chiral nanomaterials that can intercalate a large amount of guest organics in a crystal interior as well as on outer surface, and effectively exhibit a strong chiroptical response. Layered double hydroxides (LDHs) and layered hydroxide salts (LHSs), which are widely known as layered crystals of capability of intercalation/adsorption of ions and molecules, are good options for this purpose.

Herein, we demonstrate the synthesis of a nanometric nickel LHS modified with chiral amino acids on crystal surface and interlayer galleries. The obtained material was found to exhibit an induced circular dichroism (ICD) at the wavelength of *d-d* transitions of Ni(II) metal centres. The crystallization of LHS was performed in the presence of amino acids which were used to impart chiral characteristic. In contrast to conventional LDHs and LHSs as powders of micron-sized crystals, the reaction scheme developed here allows to achieve colloidal dispersion of nanocrystals; the aqua complex of Ni(II) coordinated by chiral amino acids is hydrolyzed by adding an alkalization agent, to yield Ni-LHS with a diameter of 2–3 nm, accommodating chiral amino acids in an in-situ manner. Thanks to the nanometric nature, the present Ni-LHS nanocrystals can be homogeneously dispersed in a solvent and exhibit strong ICD in the spectral range of *d-d* transitions of Ni(II) metal centres. The capability of loading additional guest molecules on surface and interlayer galleries of the obtained Ni-LHS nanocrystals is expected to open up a novel platform for chiral sensing.

2 Experimental

2.1 Chemicals

Nickel(II) chloride hexahydrate (98.0+%), D- or L-Phenylalanine (D- or L-PHE), ethanol (EtOH, 99.5%) were purchased from FUJIFILM Wako Pure Chemicals Corp. Propylene oxide (PO, ≥ 99%) was purchased from Sigma-Aldrich Co. All the chemicals were used as received.

2.2 Synthesis of layered hydroxide salt nanocrystals

The typical synthesis of Ni-LHS nanocrystals is as follows. $NiCl_2 \cdot 6H_2O$ (0.226 g; 0.95 mmol) and D- or L-PHE (0.157 g; 0.95 mmol) were homogenously mixed in EtOH (2.50 mL; 42.8 mmol) in a closed container. (Note: PHE is not soluble in ethanol, but its Ni complex is soluble in ethanol as discussed in the Results & Discussion section). At a room temperature (20 °C), PO (1.00 mL; 14.3 mmol) was added to the mixture and further stirred for 1 min to yield a homogeneous solution. Then, stirring was stopped, and the container was kept at a room temperature (~20 °C).

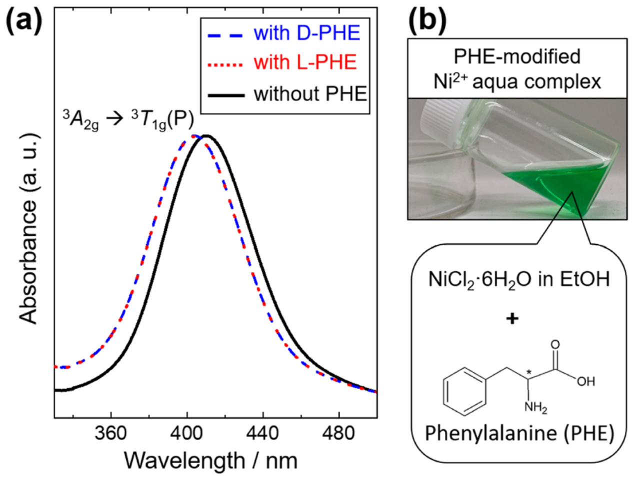

Fig. 1 **a** UV-Vis spectra of $NiCl_2 \cdot 6H_2O$ in EtOH with and without Phenylalanine (PHE). **b** photo image of the solution containing D-PHE

All the synthesis was performed under an ambient atmosphere and the reaction container was sealed throughout the reaction except when adding PO.

2.3 Characterizations

Ultraviolet-visible (UV-Vis) spectra (V-750 spectrophotometer, JASCO Corp.) of precursory solutions containing (D- or L-) PHE before the addition of PO were measured to assess the coordination environment of nickel cations. Crystalline nature of samples was identified by X-ray diffraction (SmartLab, Rigaku) using Cu Kα radiation ($\lambda = 0.154$ nm); a colloidal dispersion was poured on a petri-dish preliminarily-heated at 60 °C for the drying, and then collected powders were analyzed. The crystallite size along the c axis, out-of-plane direction of hydroxide layers, calculated from Scherrer's equation, is <3 nm. Fourier transform infrared (FT-IR) spectroscopy was carried out to analyze chemical bonds of obtained samples after drying, using a FT-IR spectrometer (ALPHA FT-IR spectrometer, Bruker Optik GmbH, Germany) by KBr pellet method. A transmission electron microscope (JEM-2000FX, JEOL, Japan) was employed to observe fine structures. For the preparation of the TEM sample, 2 μL of as-prepared colloidal dispersion was diluted with 10 mL of ethanol and then drop-casted on a Cu grid and allowed for drying. This drop-casting process was repeated five times. Thermogravimetric-differential thermal (TG-DTA) analysis (Thermo Plus Evo, Rigaku, Japan) was carried out at a ramp rate of 10 °C min^{-1} while continuously supplying air to assess the thermal behavior and chemical composition. The TG-DTA analyses were performed on samples collected by centrifugation at 50,000 rpm for 72 h (CS120FNX, Hitachi, Japan). The crystal model of Fig. 3c was produced by using VESTA software [23].

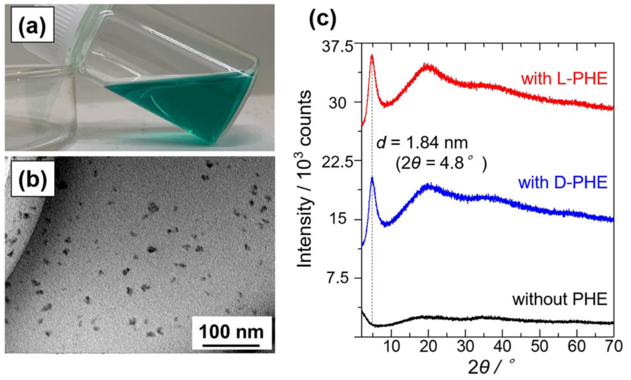

Fig. 2 **a** Appearance and **b** TEM image of Ni-LHS prepared with D-PHE. **c** XRD patterns of Ni-LHS prepared with and without L-/D-PHE

3 Evaluation of chiroptical property

Circular dichroism (CD) measurement was performed on a JASCO J-820 spectropolarimeter to evaluate chiroptical property of colloidal dispersion of Ni-LHS NC. The data were expressed as moler ellipticity $[\theta]$ ($deg \cdot cm^2 \cdot decimol^{-1}$) [Eq. 1]:

$$[\theta] = \frac{\theta}{10cl} \tag{1}$$

where, θ: ellipticity (mdeg), c: molality (mol/L), and l: cell length (cm). The molality corresponds to the concentration of Ni(II) in the analyte; as prepared colloidal dispersion ($[Ni^{2+}] = 0.38$ mol/L) was diluted into 2/3 and subjected to the measurement, i.e., $c = 0.25$ mol/L. $l = 1.0$ cm

4 Results and discussion

4.1 Synthesis of colloidal dispersion of chiral layered hydroxide salt

Phenylalanine (PHE), an essential aromatic amino acid in humans and also applicable to protein detection [24], was used as a chiral amino acid for the chiral modification of LHS. First, the precursory solution before adding alkalization agent was investigated. Figure 1(a) shows UV-Vis spectra of $NiCl_2 \cdot 6H_2O$ in ethanol (EtOH) with and without PHE. The blue shift of the *d-d* absorption in the cases for with PHE suggests that PHE of a higher ligand field partially replaces H_2O ligands surrounding Ni(II) in the solution; PHE: Ni = 1:1 in mole. Phenylalanine (PHE), which does not dissolve solely in ethanol, homogeneously dissolved in the presence of Ni(II), also suggesting the formation of an ethanol-philic Ni(II) aqua complex partially-coordinated by PHE (Fig. 1(b)).

To this precursory mixture, PO was added as an alkalization agent. Protonation and subsequent ring opening

Fig. 3 **a** Thermogravimetric-differential thermal analysis (TG-DTA) curves of LHS prepared with D-PHE. **b** FTIR spectra of Ni-LHS prepared with and without PHE. **c** Schematic illustration showing the structure of Ni-LHS accommodating PHE

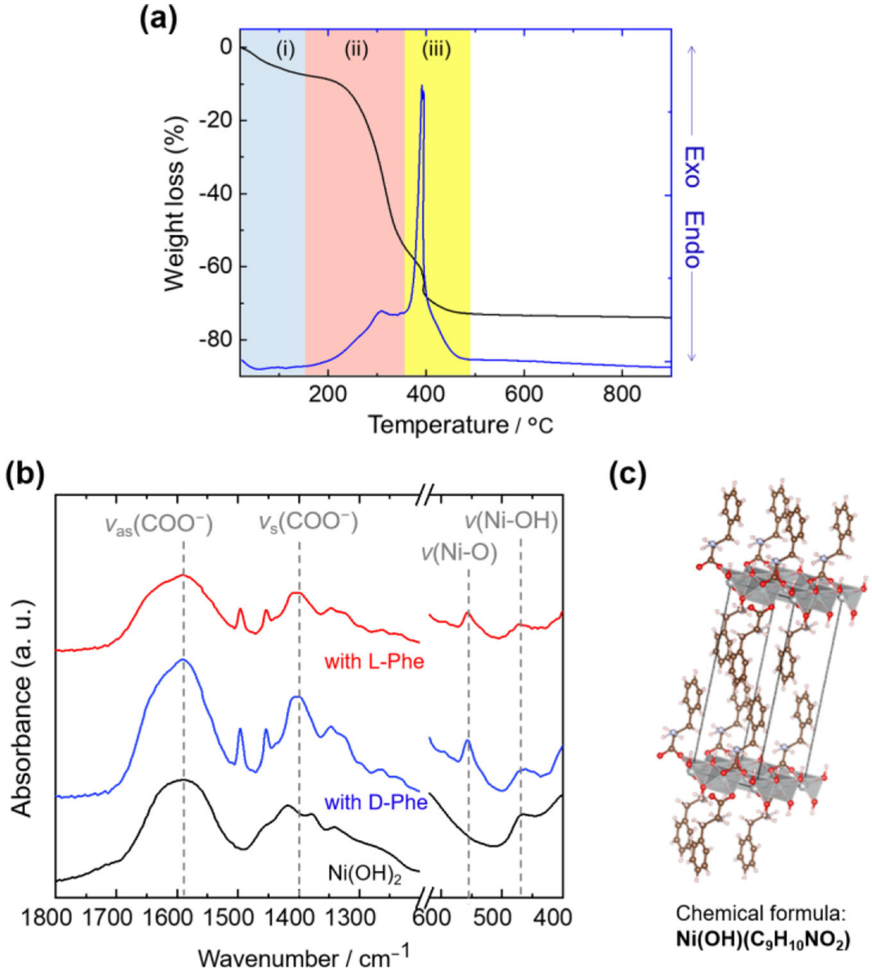

reaction of epoxides including PO is known to induce alkalization and yield metal hydroxide in an aqueous media [25–31]. This PO-driven alkalization was applied for the solution containing PHE and Ni(II) in the presence of a limited amount of H_2O (H_2O/Ni(II) = 6). Limiting the amount of water successfully prevents the release of PHE from Ni(II) aqua complex. After 24 h of the reaction, hydrolysis of the metal aqua complex led to form a clear solution (Fig. 2a). Transmission electron microscopy (TEM) revealed that a colloidal dispersion of nanoparticles with a diameter of <10 nm is formed (Fig. 2b). Phenylalanine (PHE) plays a critical role in the formation of the colloidal dispersion; indeed, gel-like solid was obtained in the case prepared without PHE (See Supporting Information Fig. S1).

Figure 2(c) shows XRD patterns of Ni-LHS prepared with and without L-/D-PHE. The referential sample prepared without PHE is ascribed to α,β-interstratified $Ni(OH)_2$ with a turbostratic disorder as is reported in a previous literature [32, 33], whereas, Ni-LHS prepared with L-/D-PHE show peaks which are indicative of α-$Ni(OH)_2$ with a layered structure. The interlayer distance is estimated to 1.84 nm from the diffraction by the basal plane. The distance is in good agreement with the one in the case of the bilayer head-to-tail arrangement of PHE molecules, with 8.3 Å in length, in the direction perpendicular to the hydroxide layer in an inclined manner. This configuration with a comparable *d* value allowing for the structurally beneficial π–π interaction has been reported for PHE accommodated in LDHs [34–36].

Figure 3(a) shows thermogravimetric-differential thermal analysis (TG-DTA) curves of Ni-LHS prepared with D-PHE. Ni-LHS suspension was centrifuged and the collected powder was analyzed. Weight losses can be ascribed to the following reactions; (i) <150 °C: desorption of physically-adsorbed water; (ii) 200–350 °C: release of water from interlayers and/or condensation of OH groups, and evaporation of D-PHE; (iii) peak at 370 °C: combustion of D-PHE in interlayer galleries. From the series of events of weight losses, Ni/PHE (mol/mol) is calculated to be 1/1 (See Supporting Information for the details).

Figure 3(b) shows FTIR spectra of Ni-LHS prepared with and without PHE. Pristine $Ni(OH)_2$ shows a broad band around at 1600 cm^{-1} corresponding to bending mode

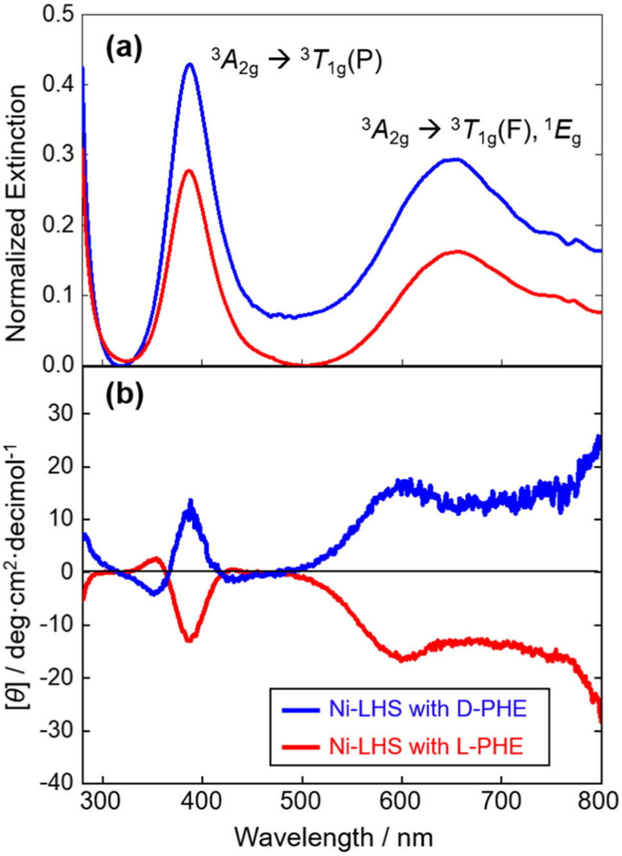

Fig. 4 **a** UV-Vis spectra and **b** corresponding CD spectra of colloidal suspensions of Ni-LHS accommodating D- and L-PHE. [*θ*]: Molar ellipticity

of water molecules [37], and a weak absorption at 472 cm^{-1} due to *ν*(Ni-OH) [38]. The coexistence of PHE leads to the appearance of additional bands. The peaks on the spectra for with PHE can be assigned as follows: 1497 cm^{-1} and 1454 cm^{-1}: CH_2 scissoring deformation; 1412 cm^{-1}: COO^- symmetric stretch ($\nu_s(COO^-)$); 1590 cm^{-1}: COO^- asymmetric stretch ($\nu_{as}(COO^-)$) [39]. The degree of splitting between $\nu_{as}(COO^-)$ and $\nu_s(COO^-)$ reflects the coordination mode of carboxylate moiety to the metal atoms [40]. A splitting of ca. 178 cm^{-1} in the present case indicates that oxygen ions of the carboxylate bind Ni(II) through a bridging coordination; adjacent Ni(II) are connected by (κ^1-κ^1)-μ_2 carboxylate group [41, 42]. The coordination through the carboxylic group is also supported by the appearance of *ν* (M-O) at 557 nm, whereas the sign of the formation of *ν*(M-N) bond typically appeared at ca. 420 nm was not observed [42]. Taking into account the results of XRD, TG-DTA, and FTIR analyses, Ni-LHS crystal prepared in the present study can be schematically described as shown in Fig. 3(c). The material obtained has a chemical composition of $Ni(OH)(C_9H_{10}NO_2)$ with a structure of stacking of the hydroxide sheets with interlayer galleries accommodating PHE with the bilayer head-to-tail arrangement.

4.2 Chiroptical response of the obtained materials

To date, the synthesis of inorganic nanoparticles, such as sulfides and metals with chiroptical properties relies on strong metal-sulfur interaction by employing cysteine as a typical additive. A characteristic feature for the synthesis in this study is that various types of chiral amino acids other than cysteine can be used to prepare inorganic nanomaterials. This is an advantageous feature to tune the surface chemistry of the obtained crystal for the application as a chiral adsorbent. Under the present solvent condition, relatively hydrophobic amino acids can be incorporated in the crystals (Table S1). The hydrophobic amino acids form stable complexes with Ni(II) in precursory ethanolic solutions as is the case for Fig. 1b which is a critical requirement to achieve the subsequent alkalization reaction to yield homogeneous colloidal dispersion of Ni-LHS nanoparticles. The synthesis of suspensions of LDH and LHS nanocrystals in various systems has been demonstrated [32, 43–46], while the introduction of chiral molecules into these suspended nanocrystals has been for the first time achieved in the present study.

Induced circular dichroism (ICD) is observed when chiral (bio-)polymers have strong and specific physical interaction with a chromophore [47]. For example, ICD was reported on colloidal cellulose crystallites adsorbing congo red [47], cellulose film adsorbing trypan blue [48]. Finally, the capability of ICD from the present Ni-LHS was closely investigated. Figure 4 shows UV-Vis and CD spectra of the colloidal dispersion of Ni-LHS accommodating D- and L-PHE. The state of colloidal dispersion of nanometric Ni-LHS allows for easy CD detection in a transmission geometry through a sample. Ni-LHS with D-/L-PHE shows light absorptions originated from PHE (< 300 nm) and *d*-*d* transitions of Ni(II) composing hydroxide sheets ($^3A_{2g} \rightarrow {}^3T_{1g}$(P), $^3A_{2g} \rightarrow {}^3T_{1g}$(F), ^1E_g) (Fig. 4a). As well as CD signal at the absorption of L-/D-PHE molecules, occurrence of ICD is clearly seen in the range of *d*-*d* transitions (Fig. 4b). It is suggested that the physical interaction between PHE and Ni (II) in LHS crystals is rather strong, inferred by the cases for ICD demonstrated for chiral polymers with an organic chromophore [47–49]. The close contact between Ni(II) (achiral chromophore) and PHE (chiral molecule) allows efficient coupling between the electric transition moments of them. Additional contribution to the chiroptical property of an anisotropic arrange of elements in crystals, for example, reported on $NiSeO_4 \cdot 6H_2O$ and α-$Ni(H_2O)_6SO_4$, [50–52], and/or a dissymmetric ligand filed well-known for tris-chelated Co(III) and Cr(III) complexes [53], are not fully ruled out in the present case. Further investigation to resolve the mechanism of chiral response is required.

The precursory Ni(II)-PHE aqua complex (before alkalization reaction by adding PO) also exhibits CD signals (Fig. S2), however, the value of [*θ*] is smaller than that for

Ni-LHS with PHE. The development of hydroxo bridge (M-OH-M) to form LHS nanoparticles gives rise to much stronger chiral response, i.e., larger [θ]. The enhanced chiroptical response is an advantageous feature of using Ni-LHS as a host material to be modified with PHE. It has been reported that a stereoselective interaction between an adsorbed molecule and its neighbor occur on a surface of clays (montmorillonite, saponite), 2D crystals [54]. The 2D interlayer galleries in LDH crystals are desirable reaction field to accommodate chiral organics. Further study will open up LHS-based nanometric chromophore with a chiroptical response triggered by the recognition of guest molecules. The enhanced host-guest interaction was demonstrated for MgAl LDH modified with a chiral molecule [55], while, the nanometric and suspended features of crystals as well as the strong ICD originating from Ni(II) demonstrated for the present material are unique additional advantages compared with conventional LDHs and LHSs based materials.

5 Conclusion

We have demonstrated Ni-LHS crystals accommodating PHE molecules in their interlayer galleries. The synthesis was performed through a direct nano-crystallization triggered by PO-driven alkalization reaction. The carboxylic group of PHE binds to Ni(II) centre though a bridging coordination to form the layered crystal with a chemical composition of $Ni(OH)(C_9H_{10}NO_2)$ and an interlayer distance of 1.84 Å. Thanks to the strong physical interaction between PHE and Ni(II), the material exhibits ICD in the spectral range of *d-d* transitions of Ni(II). The materials developed here expectedly open up applications in which chirality is fused with advantageous features of LHS crystals.

Acknowledgements The present work is partially supported by the JSPS KAKENHI Grant Numbers JP18K19134, JP20H02442, Grant-in-Aid for Scientific Research on Innovative Areas, Grant for Basic Science Research Projects from The Sumitomo Foundation. The JSPS-CNRS bilateral program is also acknowledged for the encouragement of the discussion on the present study. Mr. T. Kurokawa is acknowledged for his help for experiments to assess reproducibility of the results.

Author contributions All authors contributed to the study conception and design. Material preparation, data collection, and analysis were performed by AK, YT, HM, and SN. The first draft of the paper was written by YT and all authors commented on previous versions of the paper. All authors read and approved the final paper.

Compliance with ethical standards

Conflict of interest The authors declare no competing interests.

References

1. Galaverna G, Corradini R, Dallavalle F, Folesani G, Dossena A, Marchelli R (2001) Chiral separation of amino acids by copper(II) complexes of tetradentate diaminodiamido-type ligands added to the eluent in reversed-phase high-performance liquid chromatography: a ligand exchange mechanism. J Chromatogr A 922(1-2):151–163. https://doi.org/10.1016/S0021-9673(01)00909-8
2. Galaverna G, Corradini R, de Munari E, Dossena A, Marchelli R (1993) Chiral separation of unmodified amino acids by ligand-exchange high-performance liquid chromatography using copper (II) complexes of l-amino acid amides as additives to the eluent. J Chromatogr A 657(1):43–54. https://doi.org/10.1016/0021-9673(93)83033-O
3. Berkessel A, Gröger H (2005) Asymmetric Organocatalysis: From Biomimetic Concepts to Applications in Asymmetric Synthesis. Asymmetric Organocatalysis: From Biomimetic Concepts to Applications in Asymmetric Synthesis. https://doi.org/10.1002/3527604677
4. Barlow SM, Raval R (2003) Complex organic molecules at metal surfaces: Bonding, organisation and chirality. Surf Sci Rep 50(6-8):201–341. https://doi.org/10.1016/S0167-5729(03)00015-3
5. Fu Z, Yin D, Xie Q, Zhao W, Lv A, Yin D, Xu Y, Zhang L (2004) Ti complexes assembled HMS as effective catalysts for epoxidation of alkene. J Mol Catal A: Chem 208(1-2):159–166. https://doi.org/10.1016/S1381-1169(03)00508-9
6. Halder M, Bhanja P, Islam MM, Bhaumik A, Islam SM (2018) Chiral copper-salen complex grafted over functionalized mesoporous silica as an efficient catalyst for asymmetric Henry reactions and synthesis of the potent drug (R)-isoproterenol. N J Chem 42(14):11896–11904. https://doi.org/10.1039/c8nj01745j
7. Li B, Bai S, Wang P, Yang H, Yang Q, Li C (2011) Encapsulation of chiral Fe(salan) in nanocages with different microenvironments for asymmetric sulfide oxidation. Phys Chem Chem Phys 13 (7):2504–2511. https://doi.org/10.1039/c0cp01828g
8. Das P, Kuźniarska-Biernacka I, Silva AR, Carvalho AP, Pires J, Freire C (2006) Encapsulation of chiral Mn(III) salen complexes into aluminium pillared clays: Application as heterogeneous catalysts in the epoxidation of styrene. J Mol Catal A: Chem 248(1-2):135–143. https://doi.org/10.1016/j.molcata.2005.12.023
9. Huang J, Fu X, Wang G, Miao Q, Wang G (2012) Axially coordinated chiral salen Mn(iii) anchored onto azole onium modified ZnPS-PVPA as effective catalysts for asymmetric epoxidation of unfunctionalized olefins. Dalton T 41 (35):10661–10669. https://doi.org/10.1039/c2dt30081h
10. Gheorghiu CC, Machado BF, Salinas-Martínez De Lecea C, Gouygou M, Román-Martínez MC, Serp P (2014) Chiral rhodium complexes covalently anchored on carbon nanotubes for enantioselective hydrogenation. Dalton T 43(20):7455–7463. https://doi.org/10.1039/c3dt53301h
11. Gao X, Han B, Yang X, Tang Z (2019) Perspective of chiral colloidal semiconductor nanocrystals: opportunity and challenge. J Am Chem Soc 141(35):13700–13707. https://doi.org/10.1021/jacs.9b05973
12. Ben Moshe A, Szwarcman D, Markovich G (2011) Size dependence of chiroptical activity in colloidal quantum dots. Acs Nano 5(11):9034–9043. https://doi.org/10.1021/nn203234b
13. Ben-Moshe A, Teitelboim A, Oron D, Markovich G (2016) Probing the Interaction of Quantum Dots with Chiral Capping Molecules Using Circular Dichroism Spectroscopy. Nano Lett 16 (12):7467–7473. https://doi.org/10.1021/acs.nanolett.6b03143

14. Varga K, Tannir S, Haynie BE, Leonard BM, Dzyuba SV, Kubelka J, Balaz M (2017) CdSe Quantum Dots Functionalized with Chiral, Thiol-Free Carboxylic Acids: Unraveling Structural Requirements for Ligand-Induced Chirality. Acs Nano 11 (10):9846–9853. https://doi.org/10.1021/acsnano.7b03555
15. Ben-Moshe A, Govorov AO, Markovich G (2013) Enantioselective synthesis of intrinsically chiral mercury sulfide nanocrystals. Angew Chem Int Ed 52(4):1275–1279. https://doi.org/10.1002/anie.201207489
16. Ben-Moshe A, Wolf SG, Sadan MB, Houben L, Fan Z, Govorov AO, Markovich G (2014) Enantioselective control of lattice and shape chirality in inorganic nanostructures using chiral biomolecules. Nat Commun 5. https://doi.org/10.1038/ncomms5302
17. Lieberman I, Shemer G, Fried T, Kosower EM, Markovich G (2008) Plasmon-resonance-enhanced absorption and circular dichroism. Angew Chem Int Ed 47(26):4855–4857. https://doi.org/10.1002/anie.200800231
18. Shemer G, Krichevski O, Markovich G, Molotsky T, Lubitz I, Kotlyar AB (2006) Chirality of silver nanoparticles synthesized on DNA. J Am Chem Soc 128(34):11006–11007. https://doi.org/10.1021/ja063702i
19. Guerreiro JRL, Frederiksen M, Bochenkov VE, De Freitas V, Ferreira Sales MG, Sutherland DS (2014) Multifunctional biosensor based on localized surface plasmon resonance for monitoring small molecule-protein interaction. Acs Nano 8 (8):7958–7967. https://doi.org/10.1021/nn501962y
20. Maoz BM, Chaikin Y, Tesler AB, Bar Elli O, Fan Z, Govorov AO, Markovich G (2013) Amplification of chiroptical activity of chiral biomolecules by surface plasmons. Nano Lett 13 (3):1203–1209. https://doi.org/10.1021/nl304638a
21. McPeak KM, Van Engers CD, Bianchi S, Rossinelli A, Poulikakos LV, Bernard L, Herrmann S, Kim DK, Burger S, Blome M, Jayanti SV, Norris DJ (2015) Ultraviolet Plasmonic Chirality from Colloidal Aluminum Nanoparticles Exhibiting Charge-Selective Protein Detection. Adv Mater 27(40):6244–6250. https://doi.org/10.1002/adma.201503493
22. Wu X, Xu L, Liu L, Ma W, Yin H, Kuang H, Wang L, Xu C, Kotov NA (2013) Unexpected chirality of nanoparticle dimers and ultrasensitive chiroplasmonic bioanalysis. J Am Chem Soc 135 (49):18629–18636. https://doi.org/10.1021/ja4095445
23. Momma K, Izumi F (2011) VESTA 3 for three-dimensional visualization of crystal, volumetric and morphology data. J Appl Crystallogr 44(6):1272–1276. https://doi.org/10.1107/S0021889811038970
24. Yoosefian M, Etminan N, Juan A, Mirhaji E (2020) Ultra-low concentration protein detection based on phenylalanine-Pd/SWCNT as a high sensitivity nanoreceptor. Rsc Adv 10 (5):2650–2660. https://doi.org/10.1039/c9ra09243a
25. Gash AE, Tillotson TM, Satcher JH, Poco JF, Hrubesh LW, Simpson RL (2001) Use of epoxides in the sol-gel synthesis of porous iron(III) oxide monoliths from Fe(III) salts. Chem Mater 13(3):999–1007. https://doi.org/10.1021/Cm0007611
26. Fears TM, Sotiriou-Leventis C, Winiarz JG, Leventis N (2016) Economical synthesis of vanadia aerogels via epoxide-assisted gelation of VOCl<inf>3</inf>. J Sol-Gel Sci Technol 77 (1):244–256. https://doi.org/10.1007/s10971-015-3850-x
27. Célérier S, Laberty-Robert C, Long JW, Pettigrew KA, Stroud RM, Rolison DR, Ansart F, Stevens P (2006) Synthesis of la<inf>9.33</inf>Si<inf>6</inf>O<inf>26</inf>pore-solid nanoarchitectures via epoxide-driven sol-gel chemistry. Adv Mater 18(5):615–618. https://doi.org/10.1002/adma.200501938
28. Ko JS, Chervin CN, Vila MN, Desario PA, Parker JF, Long JW, Rolison DR (2017) Electroanalytical Assessment of the Effect of Ni:Fe Stoichiometry and Architectural Expression on the Bifunctional Activity of Nanoscale Ni<inf>y</inf>Fe<inf>1-y</inf>Ox. Langmuir 33(37):9390–9397. https://doi.org/10.1021/acs.langmuir.7b01046
29. Tokudome Y (2017) Aqueous synthesis of metal hydroxides with controllable nano/macro architectures. J Ceram Soc Jpn 125 (8):597–602. https://doi.org/10.2109/jcersj2.17095
30. Oestreicher V, Dolle C, Hunt D, Fickert M, Abellán G (2021) Room temperature synthesis of two-dimensional multilayer magnets based on α-CoII layered hydroxides. Nano Mater Sci https://doi.org/10.1016/j.nanoms.2020.12.004
31. Oestreicher V, Jobbágy M (2013) One pot synthesis of Mg2Al(OH) 6Cl·1.5H 2O layered double hydroxides: the epoxide route. Langmuir 29(39):12104–12109. https://doi.org/10.1021/la402260m
32. Tarutani N, Tokudome Y, Jobbágy M, Viva FA, Soler-Illia GJAA, Takahashi M (2016) Single-Nanometer-Sized Low-Valence Metal Hydroxide Crystals: Synthesis via Epoxide-Mediated Alkalinization and Assembly toward Functional Mesoporous Materials. Chem Mater 28(16):5606–5610. https://doi.org/10.1021/acs.chemmater.6b02510
33. Rajamathi M, Kamath PV, Seshadri R (2000) Polymorphism in nickel hydroxide: Role of interstratification. J Mater Chem 10 (2):503–506. https://doi.org/10.1039/a905651c
34. Marek AA, Verney V, Taviot-Gueho C, Totaro G, Sisti L, Celli A, Leroux F (2019) Outstanding chain-extension effect and high UV resistance of polybutylene succinate containing amino-acid-modified layered double hydroxides. Beilstein J Nanotechnol 10:684–695. https://doi.org/10.3762/BJNANO.10.68
35. Aisawa S, Sasaki S, Takahashi S, Hirahara H, Nakayama H, Narita E (2006) Intercalation of amino acids and oligopeptides into Zn-Al layered double hydroxide by coprecipitation reaction. J Phys Chem Solids 67(5-6):920–925. https://doi.org/10.1016/j.jpcs.2006.01.004
36. Aisawa S, Takahashi S, Ogasawara W, Umetsu Y, Narita E (2001) Direct intercalation of amino acids into layered double hydroxides by coprecipitation. J Solid State Chem 162(1):52–62. https://doi.org/10.1006/jssc.2001.9340
37. Zhao YL, Wang JM, Chen H, Pan T, Zhang JQ, Cao CN (2004) Al-substituted α-nickel hydroxide prepared by homogeneous precipitation method with urea. Int J Hydrog Energy 29 (8):889–896. https://doi.org/10.1016/j.ijhydene.2003.10.006
38. Aghazadeh M, Golikand AN, Ghaemi M (2011) Synthesis, characterization, and electrochemical properties of ultrafine β-Ni (OH)<inf>2</inf> nanoparticles. Int J Hydrog Energy 36 (14):8674–8679. https://doi.org/10.1016/j.ijhydene.2011.03.144
39. Li HQ, Chen A, Roscoe SG, Lipkowski J (2001) Electrochemical and FTIR studies of L-phenylalanine adsorption at the Au(111) electrode. J Electroanal Chem 500(1-2):299–310. https://doi.org/10.1016/S0022-0728(00)00391-0
40. Lausund KB, Petrovic V, Nilsen O (2017) All-gas-phase synthesis of amino-functionalized UiO-66 thin films. Dalton T 46 (48):16983–16992. https://doi.org/10.1039/c7dt03518g
41. Prevot V, Forano C, Besse JP, Abraham F (1998) Syntheses and Thermal and Chemical Behaviors of Tartrate and Succinate Intercalated Zn<inf>3</inf>Al and Zn<inf>2</inf>Cr Layered Double Hydroxides. Inorg Chem 37(17):4293–4301
42. Shamsi M, Yadav S, Arjmand F (2014) Synthesis and characterization of new transition metal {Cu(II), Ni(II) and Co(II)} l-phenylalanine-DACH conjugate complexes: In vitro DNA binding, cleavage and molecular docking studies. J Photochem Photobiol B: Biol 136:1–11. https://doi.org/10.1016/j.jphotobiol.2014.04.009
43. Murai S, Tokudome Y, Katsura R, Sakamoto H, Noguchi K, Takahashi M, Tanaka K (2020) Layered Double Hydroxide Nanosheets on Plasmonic Arrays of Al Nanocylinders for Optical Sensing. ACS Appl Nano Mater 3(6):5838–5845. https://doi.org/10.1021/acsanm.0c01001
44. Tokudome Y, Morimoto T, Tarutani N, Vaz PD, Nunes CD, Prevot V, Stenning GBG, Takahashi M (2016) Layered Double Hydroxide Nanoclusters: Aqueous, Concentrated, Stable, and Catalytically Active Colloids toward Green Chemistry. Acs Nano 10(5):5550–5559. https://doi.org/10.1021/acsnano.6b02110

45. Kino D, Tokudome Y, Vaz PD, Nunes CD, Takahashi M (2017) Synthesis of Co–Al layered double hydroxide nanoclusters as reduction nanocatalyst in aqueous media. J Asian Ceram Soc 5 (4):466–471. https://doi.org/10.1016/j.jascer.2017.10.003
46. Schneiderová B, Demel J, Pleštil J, Janda P, Bohuslav J, Ihiawakrim D, Ersen O, Rogez G, Lang K (2013) Nickel hydroxide ultrathin nanosheets as building blocks for electrochemically active layers. J Mater Chem A 1(37):11429–11437. https://doi.org/10.1039/c3ta12129a
47. Dong XM, Gray DG (1997) Induced circular dichroism of isotropic and magnetically-oriented chiral nematic suspensions of cellulose crystallites. Langmuir 13(11):3029–3034
48. Edgar CD, Gray DG (2001) Induced circular dichroism of chiral nematic. Cellul Films Cellul 8(1):5–12. https://doi.org/10.1023/A:1016624330458
49. Allenmark S (2003) Induced circular dichroism by chiral molecular interaction. Chirality 15(5):409–422. https://doi.org/10.1002/chir.10220
50. Katō T (1972) Optical Activity of Iron Group Selenate Crystals. II. Theoretical Analysis. J Phys Soc Jpn 32(1):192–201. https://doi.org/10.1143/JPSJ.32.192
51. Meredith PL, Palmer RA (1969) Vibronic structure in the circular dichroism of α-Ni(H2O)6SO4. J Chem Soc D: Chem Commun 22:1337–1339. https://doi.org/10.1039/C29690001337
52. Grinter R, Harding MJ, Mason SF (1970) Optical rotatory power of co-ordination compounds. Part XIV. Crystal spectrum and circular dichroism of α-Ni(H2O)6SO4. Journal of the Chemical Society A: Inorganic, Physical, and Theoretical Chemistry:667-671. https://doi.org/10.1039/J19700000667
53. Richardson FS (1979) Theory of Optical Activity in the Ligand-Field Transitions of Chiral Transition Metal Complexes. Chem Rev 79(1):17–36. 10.e1021/cr60317a003
54. Sato H, Hiroe Y, Tamura K, Yamagishi A (2005) Orientation tuning of a polypyridyl Ru(II) complex immobilized on a clay surface toward chiral discrimination. J Phys Chem B 109 (40):18935–18941. https://doi.org/10.1021/jp053541p
55. Wei M, Pu M, Guo J, Han J, Li F, He J, Evans DG, Duan X (2008) Intercalation of L-dopa into layered double hydroxides: enhancement of both chemical and stereochemical stabilities of a drug through host - Guest interactions. Chem Mater 20 (16):5169–5180. https://doi.org/10.1021/cm800035k